Review of Scientific Instruments

RF generation using a compact bench gyromagnetic line

Cite as: Rev. Sci. Instrum. **93**, 024704 (2022); https://doi.org/10.1063/5.0067931
Submitted: 20 August 2021 • Accepted: 12 January 2022 • Published Online: 02 February 2022

J. O. Rossi, F. S. Yamasaki, J. J. Barroso, et al.

Review of Scientific Instruments ARTICLE scitation.org/journal/rsi

RF generation using a compact bench gyromagnetic line

Cite as: Rev. Sci. Instrum. 93, 024704 (2022); doi: 10.1063/5.0067931
Submitted: 20 August 2021 • Accepted: 12 January 2022 •
Published Online: 2 February 2022

J. O. Rossi,[1,a)] F. S. Yamasaki,[1] J. J. Barroso,[1] A. F. Greco,[1] E. G. L. Rangel,[1] A. F. Teixeira,[1] L. P. S. Neto,[2] and E. Schamiloglu[3]

AFFILIATIONS

[1] National Institute for Space Research (INPE), São José dos Campos, São Paulo 12227-010, Brazil
[2] Federal University of São Paulo (UNIFESP), São José dos Campos, São Paulo 12247-014, Brazil
[3] University of New Mexico (UNM), Albuquerque, New Mexico 87131, USA

[a)] **Author to whom correspondence should be addressed:** jose.rossi@inpe.br

ABSTRACT

The search for new technologies aiming to reach radiofrequency (RF) generation in different manners for diverse ends is a constant demand for several applications. The goal is to develop cost-effective and simpler systems compared to those that already exist. Our motivation is to reach an alternative way of generating RF in pulsed transmission systems employing a gyromagnetic nonlinear transmission line (GNLTL). The GNLTL consists of a ferrite-loaded-coaxial transmission line and can produce a large frequency spectrum with RF conversion efficiency above 10% from about 200 MHz up to the frequency of 2–4 GHz (S-band) for potential space-based applications. In a GNLTL, the signal amplitude is related to its propagation velocity since the peak voltage travels faster than its portion of lower amplitudes since the ferrite permeability decreases with the current amplitude. As the pulse crest travels faster than its valley, a time reduction happens in the output rise time, called pulse sharpening. Besides, the magnetic moments of ferrite dipoles initially aligned with the axial magnetic bias are displaced from their original position by the azimuthal field generated around the inner conductor by the current pulse, resulting in a damped precession movement. This movement happens along the line length as the current pulse propagates, inducing high-frequency oscillations. In short, the paper's goal is to present the experimental results using a 60-cm gyromagnetic line to provide RF in the GHz range using a solenoid for magnetic bias on a testing bench. Finally, the paper discusses the influence of the azimuthal and the axial magnetic fields on the output signal with the ferrite rings operating in a saturation state during the current pulse propagation.

I. INTRODUCTION

There is a growing interest in searching for new technologies capable of generating radiofrequency (RF) in alternative ways in several applications.[1–3] The growing interest in these new devices is due to the search for cheaper and simpler pulsed RF sources in transmitter systems than the existing ones. The motivation for this work was to generate RF using a bench compact gyromagnetic nonlinear transmission line. In general, many published works related to this subject present results using large systems.[4–10] However, a paper published by Dolan[11] describes a high voltage generator with a variable amplitude of up to 11.5 kV used to feed a bench gyromagnetic nonlinear transmission line (GNLTL), close to the experiment developed here. He has reported that a compact gyromagnetic line system can be built on a bench, using smaller cross-section ferrite beads, with an outer diameter of a few mm and compact pulse generators of 6–12 kV. Dolan used a 72-cm long line with 20–40 kA/m of axial polarization using NiZn ferrite beads. However, this experiment only demonstrated pulse compression (pulse sharpening) without focusing on RF generation. Other similar studies also focused only on pulse sharpening, although with oscillations produced, they did not present any analysis concerning the precession effect.[12,13] On the other hand, our group here at INPE has been one of the pioneers for obtaining RF generation above 1 GHz using a bench system. The GNLTLs can produce a large frequency spectrum from 200 MHz to 4.0 GHz (S-band), with a conversion efficiency of above 10%, having potential space applications. The higher frequency oscillations with a better conversion efficiency in GNLTLs are due to the stronger ferrite permeability nonlinearity. In contrast, the lower nonlinear dielectric permittivity of the ceramic capacitors

and varactors limits the frequency band and efficiency in capacitive nonlinear lines.[14–16]

In gyromagnetic lines, the signal amplitude has a direct relation with the velocity of propagation $v(i)$, which depends on the pulse current.[17] In this way, the voltage pulse peak propagates faster than its lower portion of smaller amplitude since the ferrite permeability decreases with the pulse current $[v(i) = 1/\sqrt{\mu(i)\varepsilon}]$. Moreover, as the crest of the pulse travels faster than its base, then the velocity of propagation is increased along the rising edge and so the rise time of the output pulse is reduced, a process known as pulse sharpening.[17,18] The shock-wave formation is a harmonic generation process because of the addition of the high-frequency components to the output pulse, and relaxation or switching-time of the ferrite imposes a limit on the sharpening process.[18] However, as the crest of the pulse travels more rapidly than its base, the input pulse rise time will be reduced in the line output, also known as pulse sharpening.

The total ferrite dipole magnetic moment $\vec{M}$ initially aligned with the axial magnetic field is displaced from its original position by the azimuthal field generated around the inner conductor by the current pulse, inducing a damped precession movement around the effective field formed as shown in Fig. 1. This movement occurs along the line as the current pulse propagates and induces high-frequency oscillations on the amplitude of the output signal (see Fig. 1).

The precessional motion of the magnetization vector is described by a nonlinear evolution equation first proposed by Landau–Lifshitz in 1935,[19] which in the MKS system unit is given by

$$\frac{\partial \vec{M}}{\partial t} = -\mu_0 \gamma \vec{M} \times \vec{H}_{eff} - \frac{\alpha \gamma \mu_0}{|M|}\left(\vec{M} \times \vec{M} \times \vec{H}_{eff}\right), \quad (1)$$

where $\vec{M}$ is the magnetization vector, $\vec{H}_{eff}$ is the effective magnetic field vector, γ is the electron gyromagnetic ratio (= -1.76×10^{11} rad s^{-1} T^{-1}), α is a phenomenological gyromagnetic damping factor that depends on the material and has typical values of 0.001–0.1, and μ_0 is the vacuum magnetic permeability ($4\pi \times 10^{-7}$ H/m).

The effective field $\vec{H}_{eff}$ includes contribution from the static magnetic field $\vec{H}_0$ within the sample, the time-dependent magnetic field $\vec{h}(t)$, the anisotropy field and the exchange forces between spins, as well as stray fields.[20,21] The magnetization $\vec{M}$ represents the sum of the static magnetization $\vec{M}_0$ directed along $\vec{H}_0$ in a saturated sample when anisotropy is neglected plus a time-dependent term $\vec{m}(t)$. By scalar multiplying both sides of Eq. (1) by $\vec{M}$, we see that the magnetization magnitude remains constant in time according to the constraint $\left|\vec{M}(t)\right| = M_S$, where M_s is the saturation magnetization, such that the endpoint of $\vec{M}(t)$ moves on a sphere.[22] This constraint may be broken in certain circumstances, e.g., when the individual spins dephase during excitation, and thus $\left|\vec{M}(t)\right| = constant$ is no longer preserved. Then, the basic assumption of the Landau–Lifshitz (LL) model is not fulfilled and Eq. (1) cannot be used in such cases.[22] The first term on the right-hand side of Eq. (1) is a vector normal to $\vec{M}$ and to the field $\vec{H}_{eff}$ and accounts for the precession. The second term is also a vector normal to $\vec{M}$, but in the plane of $\vec{M}$ and $\vec{H}_{eff}$ in a direction to reduce the angle of precession. The time-dependent field $\vec{h}(t)$ in the sample is one of the unknowns of the propagation problem. The self-consistent solution of this problem requires that Eq. (1) is to be solved for $\vec{m}(t)$ in terms of $\vec{h}(t)$; this renders Eq. (1) nonlinear, whose solution $\vec{m}(t)$ is nonlinearly related to $\vec{h}(t)$ by a hysteresis loop.

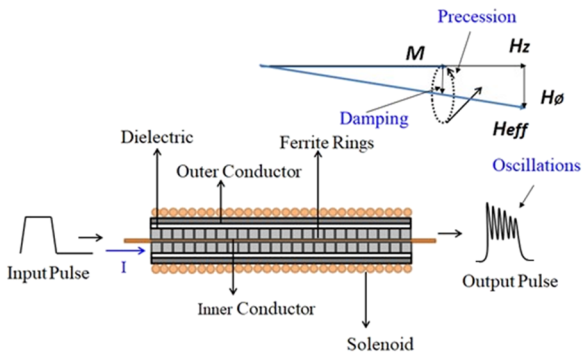

FIG. 1. Schematic of the GNLTL.

In 1955, Gilbert[23,24] demonstrated that physically implausible situations arise in the LL formulations for high values of the damping factor ($\alpha > 0.1$), showing that the LL equation is only valid in the small damping regime as discussed in Ref. 25. The distinction between LL and (Landau-Lifshitz-Gilbert) damping terms is usually insignificant for small α, although for nonconservative spin-transfer torque, for instance, this distinction becomes important even for small α.[26] Nevertheless, we can prove that LLG and LL equations are equivalent upon replacing γ in the first and second terms in (1) by $\gamma_G = \gamma/(1 + \alpha^2)$, namely,

$$\frac{\partial \vec{M}}{\partial t} = -\mu_0 \gamma_G \vec{M} \times \vec{H} - \frac{\alpha \mu_0 \gamma_G}{|M_s|}\left(\vec{M} \times \vec{M} \times \vec{H}\right), \quad (2)$$

which is the LL equation in the Gilbert form (LLG equation). Still, in the 1950s, several authors[27,28] employed analytical modeling based on the magnetic reversal switching described by the LL form equation in the Gilbert form to predict the pulse rise-time of the shock-wave front in ferrites. In 1966, Katayev[29] also presented an insightful analysis of this sharpening process using a similar method. In 1981, Weiner[30] also used Katayev's method in his modeling to predict pulse sharpening in ferrite loaded lines. Later, in the 90-decade, Perks and Dolan[31] started to use a numerical simulation based on FDTD (Finite-Difference Time-Domain) or TLM (Transmission Line Matrix) to study the pulse compression phenomena with the LL equation in the Gilbert form. Dolan[13] further used the numerical TLM simulation method to investigate the magnetic precession mechanism observed in ferrite lines that produced extremely fast rise-times when biased axially.[13] This method is quite effective in describing experimental data obtained using radial and axial H-field demagnetization factors.[11,12] More recently, there has been a growing interest in this topic because of the use of gyromagnetic lines as RF sources. Since a complex mathematical analysis is required, several recent studies[32–34] resorted to addressing this problem using numerical modeling based on Dolan's method, electromagnetic software such as COMSOL, or open-source software well established in the micromagnetic community.[35]

In the GNLTL schematic (Fig. 1), a solenoid is responsible for producing the axial magnetic field. As future work for space-based applications, our group intends to replace the solenoid in our experiment with permanent magnets (neodymium). Finally, this paper aims at presenting the experimental results using a 60-cm bench ferrite-loaded coaxial line to generate RF in the GHz range with an 80-cm long solenoid to produce the axial magnetic bias. In addition, the paper discusses the influence of the azimuthal and the axial magnetic fields on the output signal with the ferrites operating in the saturated state during pulse application.

In this paper, Sec. II presents the line construction and Sec. III describes the experimental setup used. Later, Sec. IV gives the data obtained in the tests with five modes of operation and result discussion. Finally, Sec. V reports the concluding remarks of the work.

II. GNLTL CONSTRUCTION

A GNLTL setup, established in a previous experiment developed at INPE,[36] was used. Based on several studies,[9,37,38] the NiZn ferrite beads used were from Amidon, FB-(43)-201, with outer and inner diameters of small dimensions, 1.93 and 1.09 mm, respectively, and a length of 3.8 mm. Table I shows the main properties of the material type 43 used in the ferrite bead FB (43)-201 obtained from the manufacturer.[39] According to the datasheet, this ferrite bead is lossy for RF absorption in EMI (electromagnetic interference) suppression from 20 to 250 MHz, below our operating frequency in the GHz range. Besides, in our experiment, the ferrites operate in the saturated state with lower losses since ferrite materials are very lossy at microwave frequencies below saturation.[40] In this way, the thermal issue is not a concern as we have also operated at a lower pulse repetition rate (between 1 and 10 Hz). As the intensity of the incident azimuthal field is inversely proportional to the average diameter of the ferrite, cores of small diameters are ideal for producing RF modulation on the pulse amplitude in a high-frequency band. The ferrite initial magnetic permeability given in the datasheet is of the order of 900. Ferrite beads (total of 157) inserted through an 18 AWG enameled insulated wire form the first layer of the gyromagnetic line. Two additional layers of Kapton tape wound around the ferrites keep them rigidly fixed and isolated from the ground. This structure inserted into a 3/8-in. copper tube of 60 cm, which works as ground, completes the device construction. The line extremities connected to high voltage coaxial RF connectors keep a safe connection between the generator and the attenuator without arc discharges. Figure 2 shows the ground tube and the internal line structure.

FIG. 2. Ground tube next to the internal line structure.

III. THE BENCH EXPERIMENTAL SETUP

The bench experimental setup (Fig. 3) consists of a high-voltage (HV) pulse generator from the FID-Technology manufacturer with a capacity of 12 kV/15 ns to excite the gyromagnetic line and a DC source of 30 A to feed the solenoid for axial magnetic bias generation. The HV FID pulse generator is necessary for some reasons: to provide a faster rise time to excite magnetic domains precession and a current pulse of high amplitude to generate a circumferential magnetic bias to displace the magnetization from its original position aligned with the external axial magnetic bias. In addition, it implies that magnetic domain precession is not excited if the current pulse generated is too weak because of the lower voltage applied. A DC current source generates an axial H-field between 10 and 30 kA/m using five-layers of an enameled insulated copper wire (ϕ = 1.8 mm) with 1860 turns wound on a metallic cylinder with 20-cm diameter and 80-cm length. Two HV 50-Ω 40-dB attenuators from Solar Electronics Company (2.5 kV/2.5 W) in series coupled to the 50-Ω channel input impedance of a 2.5 GHz digital oscilloscope (Agilent model DSO9104A) measure the GNLTL output pulse. Figure 4 shows the picture of the experimental testing setup built on a bench.

The system setup described previously for the output pulse measurement in the experiment considers that the line is on saturation and matched to the 50-Ω input of the attenuator. The

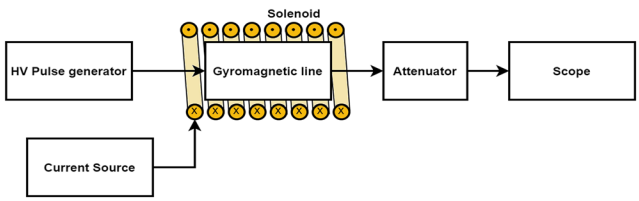

FIG. 3. Block diagram of the experimental setup used to test the GNLTL.

TABLE I. Ferrite bead 43-material specs of a std toroid at 25 °C from the Amidon datasheet.[39]

Property	Unit	Symbol	Std test conditions	Value
Initial permeability		μ_i	Freq. = 10 kHz; B < 10 G	850 ± 20%
Saturation flux density	G	B_s	H = 10 Oe	≈2950
Residual flux density	G	B_r		≈1300
Coercive force	Oe	H_c		≈0.45
Loss factor	10^{-6}	Tanδ/μi	Freq. = 1 MHz; B = 1 G	≤250
Temp. Coeff. of initial perm. (20–70 °C)	%/°C			≤1.25
Volume resistivity	Ω cm	ρ		≈10^5
Curie temperature	°C	T_c		≥135

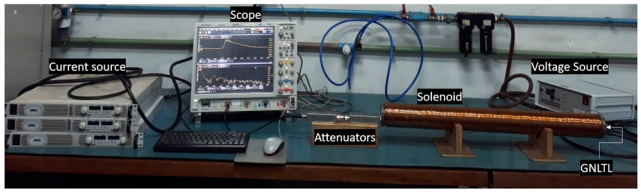

FIG. 4. Photo of the experimental setup built on a bench.

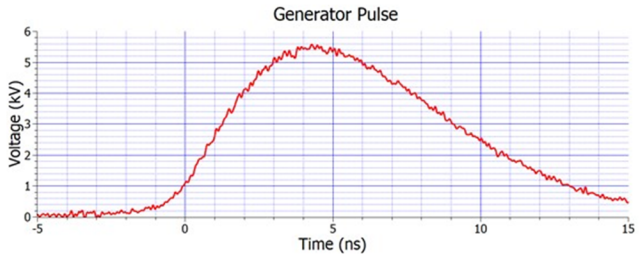

FIG. 5. Generator output pulse measured to feed the line.

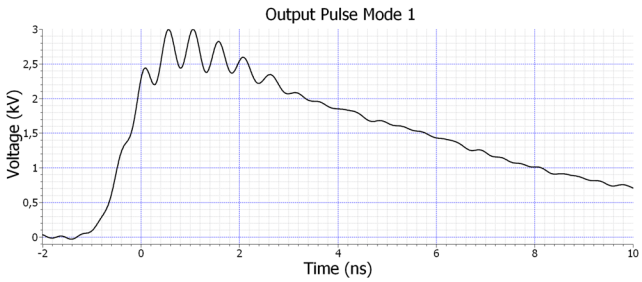

FIG. 6. Line output signal for the pulse generator set at 6.0 kV and an axial bias of 13 kA/m.

calculation for the line impedance on this condition using the formulation for saturated line inductance (L_0) in nH/m and the linear line capacitance (C_0) in pF/m gives a value of the order of 54 Ω approximately ($\sqrt{L_0/C_0}$). It means that the line mismatch can be neglected and will not affect the pulse measurements. Equations (3) and (4) below give the calculation of the saturated line inductance and linear capacitance as[41]

$$L_0 = \frac{\mu_0}{2\pi} \ln \frac{d_0}{d_i} = 422\, nH/m, \tag{3}$$

where d_o = 9.00 mm is the internal diameter of the outer conductor and d_i = 1.09 mm is the ferrite bead ring inner diameter,

$$C_0 = \frac{2\pi\varepsilon_0}{\frac{1}{\varepsilon_f} \ln\left(\frac{d_m}{d_i}\right) + \frac{1}{\varepsilon_k} \ln \frac{d_0}{d_m}} \cong 144\, pF/m, \tag{4}$$

where d_m = 1.93 mm is the outer ferrite diameter with the first term in the denominator of (4) neglected. In this case, the ferrite permittivity is ten times larger than the Kapton permittivity of the order of 4.

IV. EXPERIMENTAL RESULTS AND DISCUSSION

This section presents an experimental analysis of the 60-cm gyromagnetic line built with NiZn ferrite beads. Compared to our former work in Ref. 36, higher voltages (>5 kV) for the input pulse from the 6–12 kV FID generator were applied, increasing the azimuthal magnetic field and, thus, the oscillation frequency. Sections IV A–IV F present the input pulse waveform from the generator used to excite the GNLTL and the line operation regimes with the corresponding output waveforms and FFTs (fast Fourier transform) using a digital scope. Section IV H discusses and explains the results obtained.

A. Generator input pulse

Figure 5 shows the generator pulse measured at the output through two 40 dB attenuators connected to the 50 Ω digital scope input. The output pulse from the 6–12 kV FID generator has an asymmetric shape with adjustable amplitude starting at 6 kV, a width around 15, and a 3.0 ns rise-time. The pulse generator has a 50-Ω internal impedance to match the load.

B. Mode 1

The first mode operated at a 6.0 kV amplitude set for the generator output pulse, which results in a 3.0 kV peak with oscillations on the top (see Fig. 6) at the output with the saturated line impedance, approximately matched to the 50-Ω oscilloscope channel input. To get an axial bias field-H of about 13 kA/m, we fed the solenoid with a DC-current of about 5.5 A. The HV pulse generator injects a current pulse into the line, which excites the azimuthal magnetic field that is superposed to the axial magnetic bias H, saturating the ferrite rings and generating high-frequency oscillations that arise from the magnetic precession.

C. Mode 2

For the second operation mode, the pulse generator voltage was maintained at a 6 kV amplitude, resulting in an output peak of 3.5 kV approximately (see Fig. 7), although with an axial bias increment up to 26 kA/m approximately, which corresponds to a higher current value from the auxiliary DC source around 11 A. However, one can see in this case that no oscillations are generated around the peak pulse, as shown in Fig. 7. In this case, the explanation for this effect relies on the magnetic axial bias being so strong, which causes a smaller displacement of the ferrite magnetic moment domains from their initial alignment in the axial direction with azimuthal field applied. Therefore, the precession movement developed is weak once the precession angle is smaller. Nonetheless, as observed experimentally, if the axial bias field is not strong, the magnetic moments are weakly aligned in the axial direction, compromising the efficiency of the ferrite domain's precession movement when the incident azimuthal field is applied. From this, it is possible to conclude that there are optimum values for the incident azimuthal magnetic field and the axial magnetic bias intensities to generate the RF modulation.

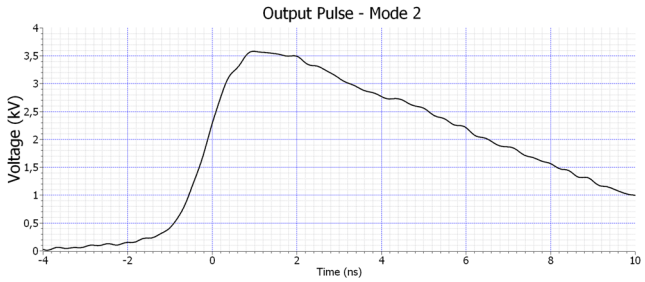

FIG. 7. Line output signal with the pulse generator set at 6.0 kV and an axial bias of 26 kA/m.

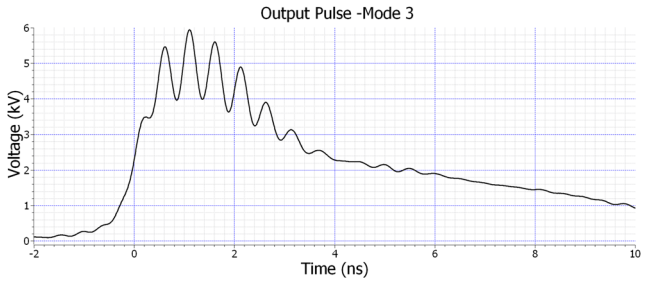

FIG. 8. Line output signal with the pulse generator set at 9.0 kV and an axial bias of 26 kA/m.

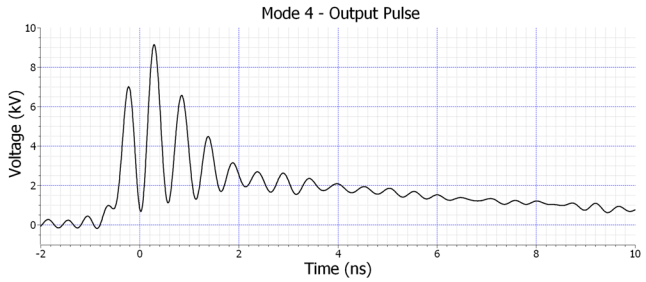

FIG. 9. Line output signal with the pulse generator set at 9.0 kV and an axial bias of 15 kA/m.

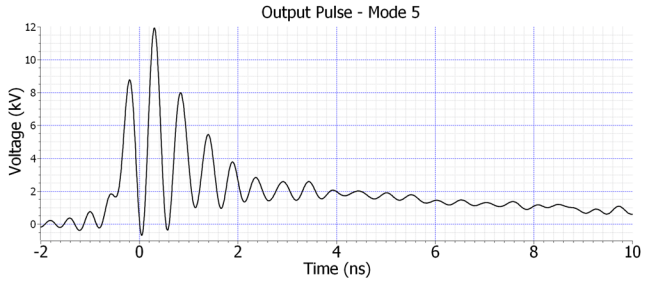

FIG. 10. Line output signal with the pulse generator set at 11.0 kV and an axial bias of 23 kA/m.

D. Mode 3

In mode 3, an applied 9 kV input pulse produces an azimuthal field of higher intensity while keeping the axial bias of 26 kA/m as in mode 2. Figure 8 shows the corresponding output pulse obtained with a peak of 6 kV and RF oscillations generated on the pulse amplitude. The idea of this mode operation was to demonstrate that the RF modulation on the output pulse can be resumed from mode 2, increasing the value of the azimuthal incident bias to compensate for the higher axial bias of 26 kA/m. Since the axial magnetic field is so strong, an azimuthal incident field of greater intensity displaces the ferrite spin moments strongly oriented in the axial direction. This explanation agrees with the discussion given in Sec. IV C.

E. Mode 4

To increase the precession angle between H_z and H_ϕ (see Fig. 1) and consequently the voltage modulation depth (VMD) of the output pulse, we kept the previous pulse generator setting at 9 kV. In addition, we decreased the solenoid current to 6.5 A (corresponding to an axial field of about 15 kA/m). Figure 9 shows the output pulse obtained with a VMD peak of about 8 kV, higher than in mode 3 with a VMD peak of only 2 kV shown in Fig. 8.

F. Mode 5

In this mode, we maximized the VMD peak by increasing the setting of the pulse generator to 11 kV and the current solenoid to 10 A (corresponding to an axial field of about 23 kA/m). Figure 10 shows the output pulse obtained with a high VMD peak of about 13 kV. Compared to the previous result (mode 4) in Fig. 9, the VMD peak increased as the azimuthal field increased further.

G. Comparison using FFT

This subsection shows a comparison of the FFTs generated by the digital oscilloscope from the output pulse measured on the five operation modes. Figure 11 shows the FFTs obtained for the five modes displayed in the same graphic for comparison. Observe that modes 1, 3, 4, and 5 FFT curves are remarkably similar between 1 and 3 GHz, showing generation of peaks around 1.9 GHz, which indicates that the ferrites are resonating at this frequency. On the other hand, comparing the FFT peaks, we can see that mode 5 has the highest amplitude peak, meaning that the RF conversion is more efficient in producing oscillations of higher VMD in this case. On the other hand, with mode 2, there is no peak around 1.9 GHz, and RF

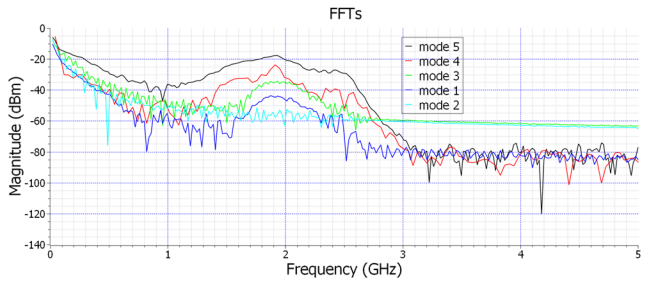

FIG. 11. FFT comparison of the five GNLTL operation modes.

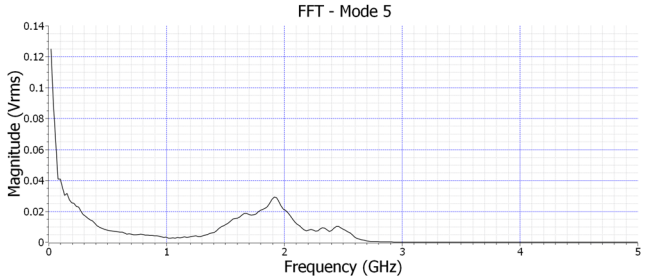

FIG. 12. FFT measured in RMS volts for mode 5.

does not occur because the axial bias intensity is much stronger than the incident magnetic field, as already explained. Figure 12 shows the FFT given in RMS voltage for mode-5 measurement of the resonance frequency of 1.92 GHz with accuracy.

H. Discussion of results

Table II summarizes the measured data for the five modes obtained as a function of the bias field H_z and azimuthal field H_ϕ in A/m. In addition, this table shows the oscillation frequency obtained from the FFT curves, the VMD peak from the output pulse waveforms, and the angle ϕ of the generated effective field H_{eff} calculated as arctan (H_z/H_ϕ). The following equations give the values of the corresponding magnetic fields:

$$H_z = \frac{NI}{l}, \tag{5}$$

where I is the solenoid current and l = 0.80 m is the solenoid length,

$$H_\emptyset = \frac{i}{\pi d_e}, \tag{6}$$

where i is the current pulse peak given by dividing the voltage peak of the output pulse on the matched load (the 50-Ω input scope channel) and d_e = 1.47 mm is the ferrite ring effective diameter given by $(d_m - d_i)/\ln(d_m/d_i)$.

From Table II, we come to two conclusions: (i) the bead-loaded section of the coaxial line resonates at 1.92 GHz because the ferrite is already on the saturation state and (ii) VMD depends on the direction of the effective field and intensities of both the fields. With the ferrite saturation, the material reaches B_s (saturation flux density) with an H-field of only 10 Oe or ~0.8 kA/m (see Table I). Thus, with the azimuthal field applied, the ferrite is already in the saturation state as the axial field is biasing the line with values much above 10 Oe. As a result, an azimuthal field increase produces no increment in frequency. Moreover, no decrease in the frequency with the axial bias happened in our experiment, which contrasts with the case reported by Romanchenko and Rostov.[42] In Rostov's experiment, probably with the coaxial line biased below the ferrite saturation, the line reached full saturation with higher azimuthal fields. We note the same phenomenon in Ulmaskulov's work[43] where the ferrite used reached saturation at an H-field axial bias of 10 kA/m. Initially, with an axial H_z = 8 kA/m and with an azimuthal field applied of about 70–80 kA/m (using their second NLTL2), they produced 2.8 GHz. However, with H_z increased to 80 kA/m, the frequency kept nearly constant at around 1.7 GHz as ferrite went on full saturation. A simple estimate in the CGS (centimeter–gram–second) system of the frequency obtained in our experiment using Kittel's formula[44] for saturated ferrite and neglecting ferrite anisotropy is

$$f = 2.8\ \text{MHz}/Oe \times \sqrt{4\pi M_s(N_x - N_z)} \times \sqrt{4\pi M_s(N_y - N_z)}, \tag{7}$$

where $B_s = 4\pi M_s$ = 2950 G and N_x, N_y, and N_z are the demagnetization factors. For the ferrite geometry of a finite cylinder, the equation below relates the three demagnetization factors as[45]

$$N_x = N_y = \frac{1}{2}(1 - N_z). \tag{8}$$

For our experiment, by assuming that N_z = 0.18, Eqs. (8) and (7) give, respectively, $N_x = N_y$ = 0.41 and f = 1.89 GHz, a value close to the one measured.

Concerning the voltage pulse modulation (VMD), ferrites are initially in the saturated state at B_s due to the axial bias. Applying the azimuthal pulse, the B_s field rotates around the direction of H_{eff} with the initial precession angle ϕ. A condition for establishing pulse modulation and consequently RF generation is by keeping a balance between both the fields by assuming equal intensities to produce a 45° angle, as shown for modes 1 and 3 approximately in Table II. Moreover, the results show that higher azimuthal field intensities enable higher induced fields along the line since pulse rate dV/dt increases as the pulse generator maintains the pulse rise time, leading to increased pulse modulation. For mode 2 in Table II, the bias magnetic field is 1.7 times higher than the pulsed azimuthal field, leading to small initial angles between the directions of H_{eff} and B_s with no pulse modulation and, consequently, no RF produced. Besides, we checked experimentally that no pulse modulation or RF is generated with a weaker axial magnetic field below 9.3 kA/m, although not shown in Table II. In this case, the initial precession angle ϕ is

TABLE II. Experimental data for the five modes.

Mode	H_z (kA/m)	$H_\emptyset$ (kA/m)	Freq. (GHz)	Input voltage (kV)	VMD output peak (kV)	Angle ϕ (degrees)
1	12.8	13.4	1.92	6.0	0.4	46.4
2	25.6	15.4	No RF	6.0	0.0	31.0
3	25.6	26.0	1.92	9.0	2.0	45.4
4	15.1	39.4	1.92	9.0	8.0	69.0
5	23.2	52.0	1.92	11.0	13.0	65.9

near 90°. A conclusion is that hard magnetization occurs and suppresses pulse modulation working with ferrite in the saturation state previously biased and with angles that are much less than 45° or near 90°. Easy magnetization happens when working with angles varying in the range of $45° \leq \phi < 90°$. The reason is that ferrites are anisotropic ferrimagnetic ceramics. For example, the easiest path of B–H curve magnetization depends on the direction of the effective H-field formed inside the material.[46] In our case, the ferrite material is on saturation, and the direction of the generated effective field affects the B_s magnetization in the ferrite. If the angle of the effective field points in the direction of easy magnetization, generated pulse modulation is higher as the B_s field aligns with H_{eff} with less resistance and smaller losses. On the contrary, if the H_{eff} angle points in the directions of harder magnetizations, B_s alignment experiences higher resistance and bigger losses, and pulse modulation can be of very low intensity or suppressed.

V. CONCLUSIONS

As shown by the results, varying simultaneously the input pulse amplitude from the HV generator to produce the incident pulsed azimuthal magnetic field and the current of the auxiliary DC source to generate the axial magnetic bias sets the intensity of the output pulse modulation. However, frequency tunability by bias field H_z was not observed as the ferrite was saturated before the application of the current pulse. On the other hand, the ferrite resonated at a frequency estimated by Kittel's formula that includes demagnetization factors for a finite cylindrical frequency. The amplitude and power of the output pulse depend mainly on the GNLTL parameters, ferrite properties, and value setting of both the fields as shown by the results for five different operation modes. Because of the ferrite anisotropy, easy and hard magnetizations led to high and low pulse modulations, respectively, depending on the precession angle. Besides, high voltage is necessary to generate intense azimuthal fields and produce a higher magnetic circumferential flux to induce oscillations with high VMD, which also depends on the value set for the axial bias. In the HV operation, the operation resonance frequency obtained for our gyromagnetic line was close to 1.9 GHz with a maximum VMD peak of the order of 13 kV. About previous studies,[42,43,47,48] the novelty here is that our line was operating at a resonance frequency because the ferrite beads used were in a saturated state at low axial fields in the range of 10–20 Oe. In addition, the considerations on material anisotropy responsible for pulse modulation depending on the initial angle of precession is a new explanation for the phenomenon observed with the ferrites operating at the resonance frequency irrespective of the amplitudes of both the fields.

ACKNOWLEDGMENTS

The authors would like to thank the National Institute for Space Research, INPE, and the Associated Plasma Laboratory, LABAP, for providing the facilities for this research study. This work was supported, in part, by CAPES (Brazil) under Grant Nos. 88887.492309/2020-00 and 88887.360820/2019-00, CNPq (Brazil) under Grant No. 306540/2019-3, FAPESP (Brazil) under Grant No. 2018/26086-2, and SOARD–AFOSR, USA, under Grant No. FA9550-18-1-0111.

AUTHOR DECLARATIONS

Conflict of Interest

The corresponding author has no conflicts of interest to disclose.

DATA AVAILABILITY

The data that support the findings of this study are available from the corresponding author upon reasonable request.

REFERENCES

[1]A. J. Fairbanks, A. M. Darr, and A. L. Garner, "A review of nonlinear transmission line system design," IEEE Access **8**, 148606–148621 (2020).
[2]E. G. L. Rangel, J. O. Rossi, J. J. Barroso, F. S. Yamasaki, and E. Schamiloglu, "Practical constraints on nonlinear transmission lines for RF generation," IEEE Trans. Plasma Sci. **47**(1), 1000–1016 (2019).
[3]D. V. Reale, J.-W. B. Bragg, N. R. Gonsalves, J. M. Johnson, A. A. Neuber, J. C. Dickens, and J. J. Mankowski, "Bias-field controlled phasing and power combination of gyromagnetic nonlinear transmission lines," Rev. Sci. Instrum. **85**, 054706 (2014).
[4]I. V. Romanchenko, V. V. Rostov, V. P. Gubanov, A. S. Stepchenko, A. V. Gunin *et al.*, "Repetitive sub-gigawatt rf source based on gyromagnetic nonlinear," Rev. Sci. Instrum. **83**, 074705 (2012).
[5]I. V. Romanchenko, V. V. Rostov, A. V. Gunin, and V. Y. Konev, "High power microwave beam steering based on gyromagnetic nonlinear transmission lines," J. Appl. Phys. **117**, 214907 (2015).
[6]M. R. Ulmaskulov, M. S. Pedos, S. N. Rukin, K. A. Sharypov, V. G. Shpak, S. A. Shunailov, M. I. Yalandin, I. V. Romanchenko, and V. V. Rostov, "High repetition rate multi-channel source of high-power rf-modulated pulses," Rev. Sci. Instrum. **86**, 074702 (2015).
[7]I. V. Romanchenko, M. R. Ulmaskulov, K. A. Sharypov, S. A. Shunailov, V. G. Shpak, M. I. Yalandin, M. S. Pedos, S. N. Rukin, V. Y. Konev, and V. V. Rostov, "Four channel high power rf source with beam steering based on gyromagnetic nonlinear transmission lines," Rev. Sci. Instrum. **88**, 054703 (2017).
[8]J. M. Johnson, D. V. Reale, J. T. Krile, R. S. Garcia, W. H. Cravey, A. A. Neuber, J. C. Dickens, and J. J. Mankowski, "Characteristics of a four-element gyromagnetic nonlinear transmission line array high power microwave source," Rev. Sci. Instrum. **87**, 054704 (2016).
[9]J. M. Johnson, D. V. Reale, W. H. Cravey, R. S. Garcia, D. H. Barnett, A. A. Neuber, J. C. Dickens, and J. J. Mankowski, "Material selection of a ferrimagnetic loaded coaxial delay line for phasing gyromagnetic nonlinear transmission lines," Rev. Sci. Instrum. **86**, 084702 (2015).
[10]J.-W. B. Bragg, J. C. Dickens, and A. A. Neuber, "Material selection considerations for coaxial, ferrimagnetic-based nonlinear transmission lines," J. Appl. Phys. **113**, 064904 (2013).
[11]J. E. Dolan, "Simulation of shock waves in ferrite-loaded coaxial transmission lines with axial bias," J. Phys. D: Appl. Phys. **32**, 1826–1831 (1999).
[12]J. E. Dolan and H. R. Bolton, "Shock front development in ferrite-loaded coaxial lines with axial bias," IEE Proc.: Sci., Meas. Technol. **147**(5), 237 (2000).
[13]J. E. Dolan, "Effect of transient demagnetisation fields on coherent magnetic switching in ferrites," IEE Proc.-A **140**(4), 294 (1993).
[14]L. R. Raimundi, J. O. Rossi, E. G. L. Rangel, L. C. Silva, E. Schamiloglu, and L. P. S. Neto, "RF generation at 200 MHz using a SiC Schottky diode lumped NLTL," in *2018 IEEE International Power Modulator and High Voltage Conference (IPMHVC)* (IEEE, 2018), pp. 473–476.
[15]L. C. Silva, J. O. Rossi, E. G. L. Rangel, L. R. Raimundi, and E. Schamiloglu, "Study of pulsed RF signal extraction and irradiation from a capacitive nonlinear transmission line," Int. J. Adv. Eng. Res. Sci. **5**(10), 121 (2018).
[16]L. P. Silva Neto, J. O. Rossi, J. J. Barroso, and E. Schamiloglu, "High-power RF generation from nonlinear transmission lines with barium titanate ceramic capacitors," IEEE Trans. Plasma Sci. **44**(12), 3424–3431 (2016).

[17]A. M. Belyantsev, A. V. Gaponov, E. Ya. Daume, and G. I. Freidman, "Experimental study of the propagation of electromagnetic waves of finite amplitude in ferrite-filled transmission lines," Sov. Phys. - JETP **20**(5), 1142–1149 (1965).
[18]P. W. Smith, "Nonlinear pulsed circuits," in *Transient Electronics: Pulsed Circuit Technology*, 1st ed. (Wiley, England, 2002), pp. 255–257.
[19]L. D. Landau and E. M. Lifshitz, "On the theory of the dispersion of magnetic permeability in ferromagnetic bodies," Phys. Z. Sowjetunion **8**, 153–169 (1935), in *Collected Papers of L. D. Landau*, edited by D. ter Haar (Gordon & Breach, New York, 1967), p. 101.
[20]H. Suhl and L. R. Walker, "Topics in guided wave propagation through gyromagnetic media," Bell Syst. Tech. J. **33**(5), 1133–1194 (1954).
[21]B. Lax and K. J. Button, *Microwave Ferrites and Ferrimagnetics* (McGraw-Hill, New York, 1962), pp. 162–177.
[22]J. Stohr and H. C. Siegmann, *Magnetism* (Springer Press, 2016), pp. 85–93.
[23]T. L. Gilbert, "A phenomenological theory of damping in ferromagnetic material," IEEE Trans. Magn. **40**(6), 3443–3449 (2004).
[24]T. L. Gilbert and J. M. Kelly, "Anomalous rotational damping in ferromagnetic sheets," in *Conference on Magnetism and Magnetic Materials* (American Institute of Electrical Engineers, Pittsburgh, PA; New York, 1955), pp. 253–263.
[25]J. Mallinson, "On damped gyromagnetic precession," IEEE Trans. Magn. **23**(4), 2003–2004 (1987).
[26]N. Smith, "Comment on: Adiabatic domain wall motion and Landau-Lifshitz damping," Phys. Rev. B **78**, 216401 (2008).
[27]R. Kikuchi, "On the minimum of magnetization reversal time," J. Appl. Phys. **27**(11), 1352–1357 (1956).
[28]E. M. Gyorgy, "Rotational model of flux reversal in square loop ferrites," J. Appl. Phys. **28**(9), 1011–1015 (1957).
[29]I. G. Katayev, "Electromagnetic shock waves in transmission lines containing ferrites with rectangular magnetization curves," in *Electromagnetic Shock Waves*, London (ILLIFE Books Ltd., 1966), pp. 53–75.
[30]M. Weiner, "Pulse sharpening in ferrite transmission lines," in *Proceeding of the 2nd IEEE International Pulsed Power Conference* (IEEE, 1979), pp. 91–95.
[31]R. M. Perks and J. E. Dolan, "Modelling electromagnetic shock lines using finite difference time-domain (FDTD) and transmission line matrix (TLM)-type models," in *IEE Symposium on Pulsed Power '99* (IEEE, 1999), pp. 27/1–27/4, Digest No. 1999/030.
[32]L. Huang, J. Meng, D. Zhu, and Y. Yuan, "Field-line coupling method for the simulation of gyromagnetic nonlinear transmission line based on the maxwell-LLG system," IEEE Trans. Plasma Sci. **48**(11), 3847–3853 (2020).
[33]Y. Cui, J. Meng, L. Huang, Y. Yuan, H. Wang, and D. Zhu, "Operation analysis of the wideband high-power microwave sources based on the gyromagnetic nonlinear transmission lines," Rev. Sci. Instrum. **92**, 034702 (2021).
[34]S. Y. Karelin, V. B. Krasovitsky, I. I. Magda, V. S. Mukhin, and V. G. Sinitsin, "Radio frequency oscillations in gyrotropic nonlinear transmission lines," Plasma **2**, 258–271 (2019).
[35]S. Sundara Mahalingam, B. V. Manikandan, and S. Arockiaraj, "Review-micromagnetic simulation using OOMMF and experimental investigations on nano composite magnets," in *International Conference on Applied Physics, Power and Material Science, IOP Conference Series: Journal of Physics: Conference Series* (IEEE, 2019), Vol. 1172, p. 012070.
[36]F. S. Yamasaki, J. O. Rossi, L. C. Silva, E. G. L. Rangel, and E. Schamiloglu, "Operation of a gyromagnetic line with magnetic axial bias," in *2019 IEEE Pulsed Power and Plasma Science (PPPS)* (IEEE, 2019), pp. 1–4.
[37]A. Vaselaar, "Experimental and modeling of pulse sharpening and gyromagnetic precession within a nonlinear transmission line," MS thesis, Texas Tech University, Lubbock, TX, 2011.
[38]W. Sullivan, J. Dickens, and M. Kristiansen, "Shock wave simulation of ferrite-filled coaxial nonlinear transmission lines," in *2008 IEEE International Power Modulators and High-Voltage Conference* (IEEE, 2008), pp. 517–520.
[39]See https://www.amidoncorp.com/product_images/specifications/43_Material.pdf for Amidon ferrite bead 43-material datasheet.
[40]D. M. Pozar, "Theory and design of ferrimagnetic components" in *Microwave Engineering*, 3rd ed., edited by B. Zobrist (John Wiley & Sons, 2005), p. 445.
[41]J. E. Dolan, A. J. Shapland, and H. R. Bolton, "Oil dielectric non-linear coaxial pulse sharpening lines - an evaluation," in *IEE Symposium on Pulsed Power '98* (IEEE, 1998), pp. 21/1–21/5, Digest No. 1998/258 and 1998/441.
[42]I. V. Romanchenko and V. V. Rostov, "Frequency of high-power RF-generation in nonlinear transmission lines with saturated ferrite," in *Proceedings of the 16th International Symposium on High Current Electronic*, (ICHE, Tomsk, 2010), pp. 521–524.
[43]M. R. Ulmaskulov, S. A. Shunailov, K. A. Sharypov, and M. I. Yalandin, "Multistage converter of high-voltage subnanosecond pulses based on nonlinear transmission lines featured," J. Appl. Phys. **126**, 084504 (2019).
[44]C. Kittel, "On the theory of ferromagnetic resonance absorption," Phys. Rev. **73**(2), 155–161 (1948).
[45]D.-X. Chen, J. A. Brug, and R. B. Goldfarb, "Demagnetizing factors for cylinders," IEEE Trans. Magn. **27**(4), 3601–3619 (1991).
[46]W. D. Callister, Jr., "Magnetic anisotropy," in *Materials Science and Engineering: An Introduction*, 7th ed. (John Wiley, 2007), pp. 94–95
[47]J.-W. B. Bragg, J. C. Dickens, and A. A. Neuber, "Ferrimagnetic nonlinear transmission lines as high-power microwave sources," IEEE Trans. Plasma Sci. **41**(1), 232–237 (2013).
[48]V. P. Gubanov, A. V. Gunin, O. B. Koval'chuk, V. O. Kutenkov, I. V. Romanchenko, and V. V. Rostov, "Effective transformation of the energy of high-voltage pulses into high-frequency oscillations using a saturated-ferrite-loaded transmission line," Tech. Phys. Lett. **35**(7), 626–628 (2009).